The Astrophysical Journal, 619:L187–L190, 2005 February 1

STRUCTURE IN THE ϵ ERIDANI DEBRIS DISK

J. S. Greaves,[1] W. S. Holland,[2] M. C. Wyatt,[2] W. R. F. Dent,[2] E. I. Robson,[2] I. M. Coulson,[3] T. Jenness,[3] G. H. Moriarty-Schieven,[3] G. R. Davis,[3] H. M. Butner,[3] W. K. Gear,[4] C. Dominik,[5] and H. J. Walker[6]

Received 2004 September 17; accepted 2004 December 20; published 2005 January 10

ABSTRACT

New submillimeter images have been obtained of the dust disk around the nearby K2 V star ϵ Eridani, with the total data set now spanning 5 yr. These images show the distribution of dusty debris generated by comet collisions, reflecting clearing and perturbations by planets, and may give insights to early conditions in the solar system. The structure seen around ϵ Eri at 850 μm and published in 1998 is confirmed in the new observations, and the same structure is also seen in an image obtained for the first time at 450 μm. The disk is inclined by $\approx$25° to the sky plane, with emission peaking at 65 AU, a 105 AU radius outer edge, and an inner cavity fainter by a factor of $\approx$2. The structure within the dust ring suggests perturbations by a planet orbiting at tens of AU, and long-term tracking of these features will constrain its mass and location. A preliminary analysis shows that two clumps and one arc appear to follow the stellar motion (i.e., are not background objects) and have tentative evidence of counterclockwise rotation of $\sim$1° yr^{-1}. Within the ring, the mass of colliding comets is estimated at 5–9 $M_{\oplus}$, similar to the primordial Kuiper Belt, and so any inner terrestrial planets may be undergoing an epoch of heavy bombardment.

Subject headings: circumstellar matter — planetary systems: formation — stars: individual (ϵ Eridani)

1. INTRODUCTION

Nearby solar-type stars are good targets to examine to see if the Sun's planetary system is at all typical. This involves searching not only for planets, but for extrasolar analogs of the Kuiper Belt of comets; these are detected indirectly through the dusty debris resulting from collisions. Thermal emission from this dust can be present from the mid-infrared out to millimeter wavelengths, but disks around solar-type stars are difficult to detect because sublunar masses of grains at $\lesssim$60 K produce only weak emission. Hence, the nearest disks have been imaged, first around ϵ Eridani (Greaves et al. 1998, hereafter G98), a K2 V star at 3.22 pc, and recently for τ Ceti (G8 V) at 3.65 pc (Greaves et al. 2004).[7] These are the *only* single stars comparable to the Sun within a distance of 5 pc; the only other similar (G to mid-K) stars are α Cen A and B, 61 Cyg A, and ϵ Ind A, all of which are in multiple systems where any disk can be tidally truncated. Hence comparison of the solar system to the environs of ϵ Eri and τ Ceti may shed light on the formation of planets, in particular as these stars are, respectively, younger and older. Recent Very Large Telescope Interferometer data (Di Folco et al. 2004) have demonstrated respective ages of 0.85 and 10 Gyr compared to the Sun's age of 4.5 Gyr.

Here we present new submillimeter data for ϵ Eri. The circumstellar disk has now been studied for 5 yr, with the aim of confirming its internal structure as affected by any system of planets. A longer-term goal is to eliminate background objects from features truly associated with the disk, as the latter must orbit the star and follow its proper motion. A preliminary motion study is presented here. The 850 μm images of the thermal dust emission are twice as deep as the data of G98, and a 450 μm image is shown for the first time.

2. OBSERVATIONS

The Submillimeter Common-User Bolometric Array (SCUBA) camera (Holland et al. 1999) on the James Clerk Maxwell Telescope (JCMT) was used to observe ϵ Eri between 1997 August and 2002 December. The 33.5 hr total integration comprises 56 separate images from 22 nights. The co-added data shown are for the stellar position in epoch 2002.8 of (J2000.0) R.A. = $03^{h}32^{m}55\overset{s}{.}66$, decl. = $-09°27'29\overset{''}{.}7$. The star's proper motion of $-1''$ yr^{-1} in R.A. has been corrected in the reduction using half-year ($0\overset{''}{.}5$) bins, while the total decl. shift of $0\overset{''}{.}1$ is ignored. The 850 μm FWHM beam size was $15'' \times 15\overset{''}{.}5$, with a $8'' \times 9''$ beam for the simultaneous observations at 450 μm. A 7″ Gaussian smooth was adopted to reduce the noise, for final resolutions of 17″ and 11″ at 850 and 450 μm, respectively, or 55 and 35 AU at 3.22 pc distance.

The data reduction is described in G98, but here we used the "median" gridding method of SURF (Jenness et al. 2002). Atmospheric correction was from 850 μm skydips with standard extrapolation to 450 μm. Calibration maps were made on planets and secondary calibrators, giving flux conversion factors (volts to jansky) for a 1′ diameter circular aperture. The means of these factors agree with standard values within 5%, with internal dispersions of $\pm$5%–15% (highest at 450 μm). The mean pointing drift per map was $2\overset{''}{.}7$ (maximum of $6\overset{''}{.}7$); this was linearly corrected in software and the final error is expected to be small, with random drift directions largely canceling out. Each bolometer and map was weighted according to its noise levels; the data since 2000 account for 80% of the final 450 μm image, utilizing a new filter with higher throughput. Photospheric signals of 1.7 and 6 mJy at 850 and 450 μm, respectively, were subtracted using a scaled beam map (G98);

[1] Physics and Astronomy, University of St. Andrews, North Haugh, St. Andrews, Fife KY16 9SS, UK; jsg5@st-andrews.ac.uk.
[2] UK Astronomy Technology Center, Royal Observatory, Blackford Hill, Edinburgh EH9 3HJ, UK.
[3] Joint Astronomy Center, 660 North A'ohō kū Place, University Park, Hilo, HI 96720.
[4] Department of Physics and Astronomy, Cardiff University, P.O. Box 913, Cardiff CF2 3YB, UK.
[5] Sterrenkundig Instituut "Anton Pannekoek," Kruislaan 403, 1098 SJ Amsterdam, Netherlands.
[6] CCLRC, Rutherford Appleton Laboratory, Chilton, Didcot, Oxon OX11 0QX, UK.
[7] The image for the G2 V star HD 107416 (Williams et al. 2004) demonstrates disk structure that can be resolved as far as 28.5 pc.

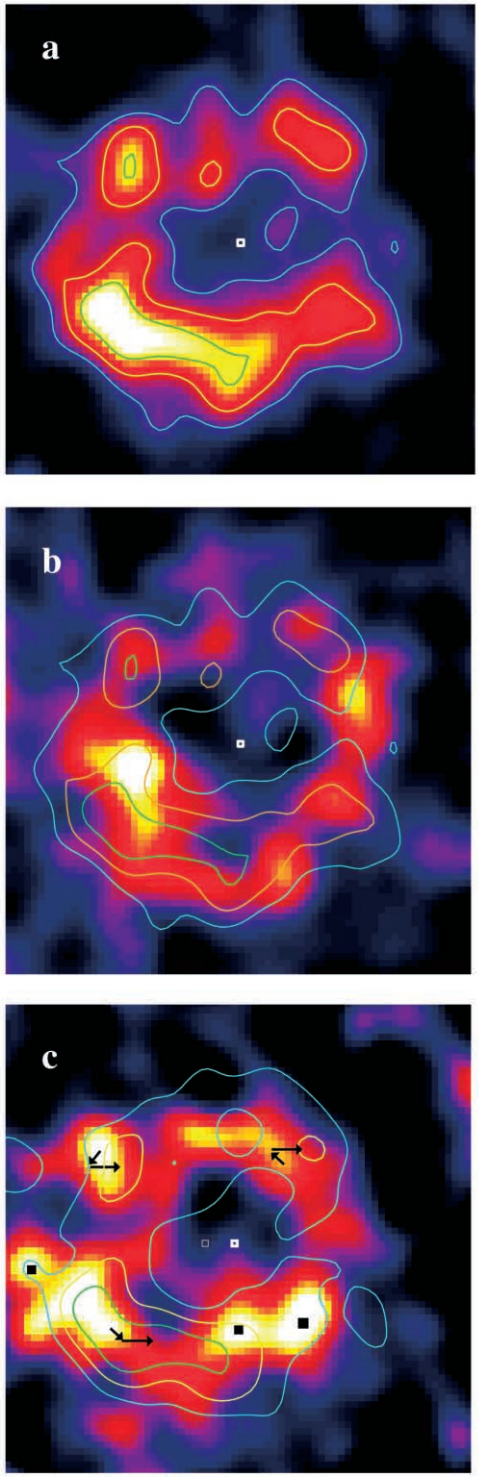

FIG. 1.—Results for the ϵ Eri dust disk. (*a*) Entire 850 μm data set, showing 1″ pixels in a 70″ field in R.A., decl. coordinates (north is up, east is left) centered about the star (*white square*, epoch 2002.8). Flux scale is linear from 0 to 5.4 mJy beam^{-1} (90% of the peak); contours are 5, 8, and 11 σ, where 1 σ is 0.5 mJy beam^{-1}. (*b*) Entire 450 μm image, showing flux from 0 to 20 mJy beam^{-1} (90% of peak), overlaid with the 850 μm contours from (*a*). (*c*) 850 μm data from 1997/8 (color scale) with superposed 30%, 50%, and 70% contours from the 2000–2002 data, in a fixed coordinate frame. The unfilled white square shows the star's position backtracked by 4.5 yr for demonstration purposes. Black squares are suggested background features, and black arrows are motion associated with the disk (see text).

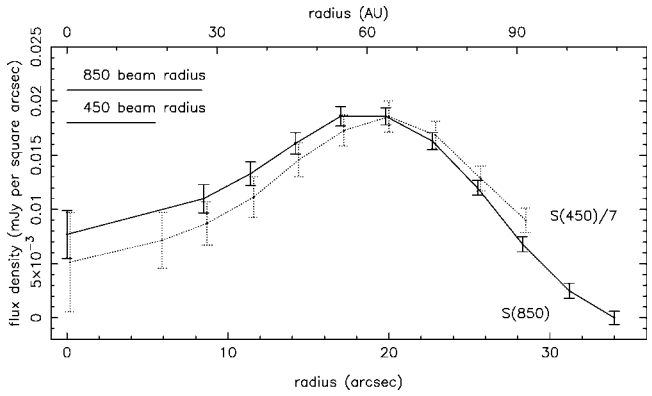

FIG. 2.—Radial profiles of the dust emission. Each point represents the mean signal within an elliptical ring, plus a point is plotted for the beam toward the star. The ring at the 20″ semimajor axis (position angle 130° east of north) joins the peaks of the brightest clumps and is centered 2″ east of the star; other rings of 2.″8 width are nested inside and outside this. The ring signals are not independent because they are less than a beam apart. Error bars are derived from the noise and number of independent beams around each ellipse. The 450 μm signal has been divided by 7 to normalize it to the 850 μm profile.

errors in these values are 10% and 30%, respectively, of the dust signal in the central beam.

The noise has been estimated from scatter in areas of the frame that have no obvious sources. At 850 μm the standard deviation of signal per 17″ beam is 0.5 mJy, while at 450 μm it is 3 mJy per 11″ beam.[8] The mean background level is not exactly zero: at 850 μm the correction is $\lesssim$0.1 mJy beam^{-1}, while at 450 μm the baseline lies at $\sim$+0.5 mJy beam^{-1}. Baselines are also not perfectly flat, so that relative flux differences of less than 15% between bright disk regions could be unreliable. Because these effects could arise from background objects seen with low significance, we chose not to subtract baselines. At 850 μm roughly one-third of beams contain a 0.5 mJy distant galaxy (Scott et al. 2002); chopping between these yields a fluctuation of $\approx$0.3 mJy that contributes significantly to our measured noise of 0.5 mJy beam^{-1}. Several probable background objects are seen within the full fields (2.′25–2.′5 across), with flux densities up to 3 and 12 mJy beam^{-1} at 850 and 450 μm, respectively.

3. RESULTS

The disk images and profiles are shown in Figures 1–3. The overall dimensions are very similar to the 850 μm image of G98, and the morphology is a ring with a central cavity seen roughly face-on. An ellipse passing through the 850 μm brightness peaks gives a good fit, with major and minor diameters of 41″ and 37″ and the longer axis oriented southeast to northwest. For a thin ring the implied inclination is $\approx$25° from the sky plane; the likely error in the dimensions is $\approx$1″ translating to $\pm$3°. A fit to the 450 μm ring is similar at $\approx$42″ $\times$ 38″, oriented slightly more north-south. In both cases, the fitted ellipse appears slightly offset, centered $\approx$1.5″–2″ east of the star; such asymmetry can be produced where there is a forced eccentricity in the dust grain orbits (Wyatt et al. 1999).[9]

Radial profiles (Fig. 2) have been derived using nested el-

[8] Per beam signals are measured within circular apertures to the FWHM of 17″ and 11″, i.e., over beam areas of 225 and 95 arcsec^2; the corresponding areas for a Gaussian beam profile are 260 and 110 arcsec^2.

[9] First-order theory predicts that the planet orbiting at 3.4 AU with e = 0.6 (Hatzes et al. 2000) would force an eccentricity of 0.04 on planetesimals at 60 AU, resulting in a net offset of 2.5 AU or 0.″75.

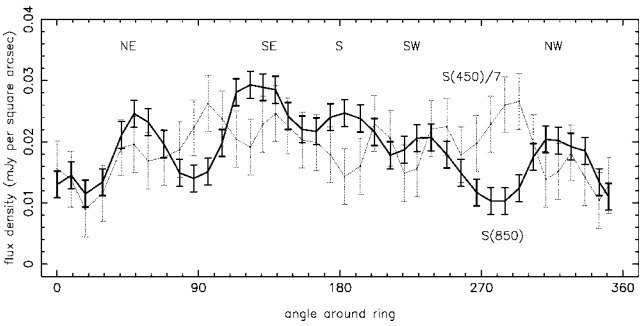

FIG. 3.—Azimuthal profiles of the dust emission, with the main flux peaks labeled; the 450 μm profile has been divided by 7 for clarity. Angles increase counterclockwise from zero at north. Points are measured along an ellipse of the semimajor axis 20″ at position angle 130°, centered 2″ east of the star, and are 3″ apart (hence not independent). Error bars correspond to the noise per beam in the smoothed images. The image baselines are not perfectly flat, contributing azimuthal variations around the ring estimated at 15% of the peak signals.

liptical annuli, and the dust ring peaks at close to 20″ (65 AU) at both wavelengths. The lower-resolution 850 μm profile is slightly more "pulled in" toward the star, but the difference is small, indicating a central cavity that is well resolved (Dent et al. 2000). The width of the higher-resolution 450 μm profile, deconvolved from the beam size, indicates that dust half as bright as the peak emission lies at 40–90 AU (12″–28″) from the star. The outer edge declines rather steeply with a cutoff at ≈32″ or 105 AU in the 850 μm data (the 450 μm profile here is affected by background objects). These dimensions are somewhat larger than inferred for Kuiper Belt dust (Liou & Zook 1999), where there is a cavity to about 25 AU and an outer edge at about 48 AU that may be associated with Neptune's 2 : 1 resonance (Levison & Morbidelli 2003).

The total dust flux within a 1′ diameter circle is 37.0 ± 2.5 mJy at 850 μm and 250 ± 20 mJy at 450 μm, in good agreement with the G98 values of 40 ± 3 and 185 ± 103 mJy. The errors quoted are from the noise over the number of included beams, added in quadrature with a 5% uncertainty in calibration (described above). The uncorrected background levels could contribute approximately ±1.25 mJy at 850 μm and +15 mJy at 450 μm. Sheret et al. (2004) have modeled the spectral energy distribution (using preliminary fluxes differing by ≈10%) and find that the dust grains should be solid rather than porous and exceed 3.5 μm in size. A simpler graybody fit yields a typical $T_{\rm dust}$ of 55 K, emissivity index of 1.0, and for an opacity of 1.7 cm^2 g^{-1} a resulting dust mass of 0.002 $M_\oplus$ (less than in G98, where $T_{\rm dust}$ was assumed to be 30 K). These values agree well with a spectral fit extending to 1.2 mm data from which Schütz et al. (2004) found 0.0017 $M_\oplus$, 50 K dust, and grains larger than 8 μm. In the context of similar stars with debris, there are now good mass estimates for four F2–K2 objects whose ages are within a factor of 2 of 1 Gyr (Sheret et al. 2004; Wyatt et al. 2005); the dust masses range from 0.0005 to 0.04 $M_\oplus$, placing ϵ Eri in the midrange.

3.1. *Structure of the Disk*

An inner planet is known from radial velocity measurements (Hatzes et al. 2000), on an orbit with an estimated semimajor axis of 3.4 AU with eccentricity of 0.6. This planet will never exceed 5.5 AU (1.″7) from the star, so little information about its environment can be gathered with our resolution, even though our data span nearly a 7 yr orbital period. However, the planet is expected to eject particles that spiral inward near its orbit, and Figure 2 shows that the center is indeed relatively clear of dust, dropping to half or less of the peak signals seen in the ring. Unlike in the 850 μm profile of G98, the signal does not rise again at small radii. The G98 central data point was probably erroneous in that the error was underestimated, being derived from the average of only 5 pixels with fortuitously close values. Figure 2 is more realistic and does not attempt to derive a central profile on scales smaller than the beam. Within this central beam, the 850 μm signal is 1.6 ± 0.6 mJy in the post-2000 data, not significantly discrepant from 2.6 ± 0.8 mJy in the 1997/1998 image.

To study the ring's internal structure it is essential that the features described be reliable and reproducible. With limited data, G98 claimed only the peak southeast of the star as clearly real, appearing in most individual maps. Now the larger data set shows that enhancements to the southwest, northwest, and northeast are also reproduced,[10] along with the arc along the south side of the ring (Fig. 1*a* and azimuthal profile in Fig. 3). Independent confirmation comes from the new 450 μm image in which these clumps are again seen at relative offsets of 2″–5″ (Fig. 1*b*). The 450 : 850 μm flux ratio is roughly constant, apart from the 450 μm peak west of the star coincident with a dip in 850 μm emission—this clump is currently unexplained but does have a close counterpart in the 350 μm image of Wilner et al. (2003). For a final check, the 850 μm data set was divided into halves to determine positional errors. Offsets of 3″–5″ between half–data sets imply errors of 1.″5–2.″5 in the final image (slightly worse between the new and G98 data, as the latter has only one-third of the total weight). Positional uncertainties are expected to be roughly (beam diameter/significance), or 2″–3″ for the 850 μm clumps at 5–9 σ above the interclump level, and 2″–5″ at 450 μm at 2–5 σ.

The 850 μm image is sufficiently deep that peaks apparently part of the ring could in fact be distant galaxies, lying behind the ring by chance. Eliminating these is important for an interpretation of the true clumps as perturbations by a planet. Genuine ring features should both move with the proper motion of the star and rotate at orbital periods of ≈280–520 yr if linked to a planet at ≈40–60 AU. During the 5 yr time span of the present data, these effects are small and comparable to the random differences. Hence we present only a preliminary analysis, seeking to identify consistent movements of several clumps.

Figure 1*c* shows comparisons[11] of the 1997/8 and 2000–2002 data sets at 850 μm; the observations were bunched in time with midpoints about 4.5 yr apart, for a stellar shift in R.A. of −4.″5. Rotation in this time should not exceed 6° or 2″ at 20″ radius. A fixed sky frame is shown in which the disk will translate to the right plus the clump features will rotate, while background galaxies will not move. (There may be ambiguous features from chance blends of ring and background features.) Figure 1*c* confirms that most of the emission is in fact associated with ϵ Eri. The earlier data clearly show the ring farther to the left and centered around the earlier stellar position. However, three flux peaks (*black squares*) appear not to have moved,

[10] Flux densities at 850 μm for these peaks are 6.7 (southeast), 4.8 (southwest), 4.7 (northwest), and 5.6 (northeast) mJy beam^{-1}. The 1.2 mm image of Schütz et al. (2004) shows somewhat different peaks but at significance only up to 4.4 σ, below our lowest contour; their image does confirm a disk extending to at least 90 AU radius.

[11] The color scale used is intended to highlight the peaks, and color transitions (e.g., red to yellow) occur over only 10% of the flux range shown. Hence, small variations in clump shapes apparent to the eye are not significant. Small differences to the image of G98 are also only functions of the color scale.

as the contours and color scale match closely, suggesting that these are background sources. Arrows mark three other features that appear both to have moved and, tentatively, to have rotated about the star by ~6° counterclockwise. While this is not definite given the positional uncertainties, it is a consistent pattern. It is also notable that rotation in the *opposite* sense plus the proper motion would give a poor alignment of the color-scale peaks and contours. We thus suggest that the northeast and northwest peaks and southeast-to-south arc are real ring features, while other clumps are either background sources or ambiguous.

4. DISCUSSION

The new images of the ϵ Eri dust ring confirm its structure and dimensions, and the addition of 450 μm data gives independent confirmation of the clumps. A pattern is tentatively identified in which two clumps and an arc appear to orbit counterclockwise about the star. A detailed model is required to identify planetary resonances (Wyatt 2003), but the motion is similar to predictions of $0\overset{\circ}{.}7$–$1\overset{\circ}{.}3$ yr^{-1} (Quillen & Thorndike 2002; Ozernoy et al. 2000). Confirmation will need a data set at least 10 yr long (when the clumps rotate beyond the 1997/8 positional errors) or images at higher resolution. The best constraint is on the *minimum* orbit size of a planet: a body inside 20 AU would force rotations greater than 15° between the data sets 4.5 yr apart, greater than the proper-motion shift already seen.

The inner planet may contribute to central clearing and also force a center offset on the ring. A second planet provides the only good explanation for the ring's substructure and must orbit at tens of AU to have a strong perturbing effect. The scale of the planetary system may be larger than the Sun's, where Neptune at 30 AU is the most distant large planet; also ϵ Eri's inner planet is more eccentric and massive than Jupiter ($\approx 2M_{\rm Jup}$ if coplanar with the disk). There is no evidence yet for terrestrial planets, but Jones (2003) argues that orbits would be stable in the habitable zone, in spite of the eccentric inner giant.

Any such terrestrial body is likely to be in an era of heavy bombardment akin to that experienced by the Earth for its first 0.6 Gyr (Maher & Stevenson 1988)—ϵ Eri is currently 0.85 Gyr old (Di Folco et al. 2004). The perturbations of the comet belt by the outer planet could result in objects falling inward and crossing orbits near 1 AU. Such infalling bodies have been inferred from transient spectral lines toward young stars such as β Pictoris (Thébault & Beust 2001), while in the solar system, planetesimals perturbed by the formation of Uranus and Neptune may have impacted the Moon as late as at 0.7 Gyr (Levison et al. 2001). For ϵ Eri, the dust alone comprises one-sixth of a lunar mass—infall of some of this icy debris could supply oceans to a habitable world, but heavy impacts might be inimical to life emerging. The generation of dust particles in a collisional cascade allows an estimate to be made of the mass in the parent comets, as described by Wyatt & Dent (2002), and for ϵ Eri we estimate 5–9 $M_\oplus$ in bodies up to a size of 10–30 km. This is somewhat dependent on the numbers of infrequently colliding largest objects, but at least 2 $M_\oplus$ will reside in bodies up to 1 km across, even if larger bodies are relatively rare (Jura 2004). These values are comparable to the 10 $M_\oplus$ estimated for the Kuiper Belt (Morbidelli et al. 2003) at early times, suggesting that ϵ Eri's disk may indeed be a close analog to the young solar system. Finally, Kenyon & Bromley (2004) have shown that distant Pluto-like bodies could still be forming at ~1 Gyr, so the planetary system will still be evolving. Further observations toward ϵ Eri will shed light on the final stages of planet formation and evolution around Sunlike stars.

We thank Ben Zuckerman for many useful discussions and the Royal Astronomical Society for the support of J. S. G. with the Sir Norman Lockyer Fellowship. The JCMT is operated by the UK Particle Physics and Astronomy Research Council, the National Research Council of Canada, and the Netherlands Organization for Pure Research. Facilities: JCMT (SCUBA).

REFERENCES

Dent, W. R. F., Walker, H. J., Holland, W. S., & Greaves, J. S. 2000, MNRAS, 314, 702
Di Folco, E., Thévenin, F., Kervella, P., Domiciano de Souza, A., Coudé du Foresto, V., Ségransan, D., & Morel, P. 2004, A&A, 426, 601
Greaves, J. S., Wyatt, M. C., Holland, W. S., & Dent, W. R. F. 2004, MNRAS, 351, L54
Greaves, J. S., et al. 1998, ApJ, 506, L133 (G98)
Hatzes, A. P., et al. 2000, ApJ, 544, L145
Holland, W. S., et al. 1999, MNRAS, 303, 659
Jenness, T., Stevens J. A., Archibald, E. N., Economou, F., Jessop, N. E., & Robson, E. I. 2002, MNRAS, 336, 14
Jones, B. W. 2003, Astron. Geophys., 44, 2.10
Jura, M. 2004, ApJ, 603, 729
Kenyon, S. J., & Bromley, B. C. 2004, AJ, 127, 513
Levison, H. F., Dones, L., Chapman, C. R., Stern, S. A., Duncan, M. J., & Zahnle, K. 2001, Icarus, 151, 286
Levison, H. F., & Morbidelli, A. 2003, Nature, 426, 419
Liou, J.-C., & Zook, H. A. 1999, AJ, 118, 580
Maher, K. A., & Stevenson, D. J. 1988, Nature, 331, 612
Morbidelli, A., Brown, M. E., & Levison, H. F. 2003, Earth Moon Planets, 92, 1
Ozernoy, L. M., Gorkavyi, N. N., Mather, J. C., & Taidakova, T. A. 2000, ApJ, 537, L147
Quillen, A. C., & Thorndike, S. 2002, ApJ, 578, L149
Schütz, O., Nielbock, M., Wolf, S., Hennin, Th., & Els, S. 2004, A&A, 414, L9
Scott, S., et al. 2002, MNRAS, 331, 817
Sheret, I., Dent, W. R. F., & Wyatt, M. W. 2004, MNRAS, 348, 1282
Thébault, P., & Beust, H. 2001, A&A, 376, 621
Williams, J. P., Najita, J., Liu, M. C., Bottinelli, S., Carpenter, J. M., Hillenbrand, L. A., Meyer, M. R., & Soderblom, D. R. 2004, ApJ, 604, 414
Wilner, D. J., Dowell, C. D., Holman, M. J., & Kuchner, M. J. 2003, BAAS, 203, 130.03
Wyatt, M. C. 2003, ApJ, 598, 1321
Wyatt, M. C., & Dent, W. R. F. 2002, MNRAS, 334, 589
Wyatt, M. C., Dermott, S. F., Telesco, C. M., Fisher, R. S., Grogan, K., Holmes, E. K., & Piña, R. K. 1999, ApJ, 527, 918
Wyatt, M. C., Greaves, J. S., Dent, W. R. F., & Coulson, I. M. 2005, ApJ, in press